Synchronization & Oscillations in the visual cortex: a Stochastic Model using a Spike Memory term

Mathilde Mougeot

ENS Cachan, CMLA, DIAM 61 avenue du Président Wilson 94235 Cachan cedex France
Université ParisX, SEGMI, 200 avenue de la République 92001 Nanterre cedex France
mougeot@cmla.ens-cachan.fr

Abstract

This study presents a model, inspired from the biology of the cortex, which reproduces the synchronization and oscillation properties of the visual cortex, for neurons in different hemispheres. A network architecture is presented which models part of the retina and parts of two visual cortical areas in opposite hemispheres. A probabilistic model is proposed to simulate the behaviour of neurons, which takes into account both spatial and temporal integrations with interneural delays, comparable to interhemispherical connectivity. Cell membrane characteristics are modeling using for each neuron a spike memory term. Neuron states are binary $\{0,1\}$, and dynamic is stochastic.

1   Introduction

A number of recent studies in the cat visual cortex have demonstrated the existence of synchronization of firing between neurons of different areas associated with the same stimulus [3] [7]. Neurons from different hemispheres with overlapping receptive fields and similar orientation selectivities tend to show synchronized firing with a temporal jitter of a few milliseconds.

The visual information from the retina to the cortex comes through a large number of cells (bipolar, ganglion, LGN and then cortical cells). The average latency of the responses of cortical cells in V1, activated by visual stimulus, is of the order of 50ms. Moreover, the visual information takes different visual pathways from retina to left or right hemispheres and different transmission delays from retina to right or left hemispheres, du to these different physical pathways can also be observed.

This model reproduces synchronization observed by the neurophysiologist J. Bullier and his team [7], for cells of different hemispheres, receiving similar information from the retina but with different temporal delays.

Different models have already been proposed in the litterature to explain synchronization or oscillations in the visual cortex [4], such as differential equations [1] or integrate and fire neurons [2] [6]. In several of these models, global connections are used to synchronize the oscillators. In our model, oscillations between cells are not a consequence of the intrinsinc periodicity of particular neurons such as pacemaker neurons [8] and synchronization between cells depends not only on well chosen delays between cells, but mostly on an internal parameter linked to spike memory, which is similar to the evolution of calcium channels.

2 Network Architecture and connectivity

• The neural net is composed of 3 layers of neurons (figure 1). Layer 1 models a part of the retina that receives images of the external world. It corresponds to the set of receptive fields of the network. Layers 2L and 2R model intermediate areas in the Left or Right visual pathways, between the retina and cortical layers. Areas 3L and 3R model small parts of Left and Right hemispheres in areas 17 of the visual cortex.

Figure 1: Architecture of the 3-layers network. Each two-dimentional layer contains many cells. Arrows represent connections between layers. Each cell also provides inputs to many cells of the following layer. Lateral connections (within a layer) are not indicated here.
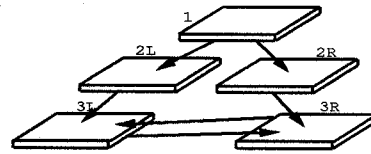
• The synaptic organization of the network is initially imposed by biological constraints. Our network, like most biological networks, is not fully connected. In each layer (except layer 1), a cell receive inputs from a set of cells of other layers via connections. For simplification, the spatial distribution of connections is randomly chosen among layers, using uniform distributions. In each layer, the proportion of connections received by a cell from cells of other layers (or of its own layer) is fixed. Two cells of a particular layer are not necessarily connected to the same cells, but receive globally the same number of connections respectively from the three other layers (previous, opposite and itself). Cells from area 3L and 3R share more or less the same receptive field, in layer 1. In figure 1, vertical arrows correspond to thalamic inputs. Horizontal arrows, which link layers 3L and 3R, model the cortico-cortical connections, that come through the corpus callosum.

• In biological systems, information is transmitted with temporal delays depending on the chosen pathways. There is no biological evidence to consider that the sum of all transmission delays between retina to left or right hemispheres are exactly the same: transmission delays depend on the crossed areas.

In our model, cells of layers 3L and 3R receive common information from layer 1, but with different temporal transmission delays ($\delta_{3L,1} \neq \delta_{3R,1}$; $\delta_{A,B}$ is the temporal delay between layer A and B) to take into account biological observations.

The delays in the model have been chosen to be consistent with neurobiological data. Visual transmission from retina to cortical area takes 50 ms. The delays have been chosen in order to have $\delta_{3L,2L} + \delta_{2L,1} = 50ms$ and $\delta_{3R,2R} + \delta_{2R,1} = 50ms + \epsilon$ with $\epsilon = 5ms$. The transmission delays between the corpus callosum, $\delta_{3L,2L}$ and $\delta_{3R,2R}$, are equal to a few ms, usually from 5 to 15 ms.

3 Dynamic

A probabilistic model is proposed to model the neurons' behaviour. This model takes into account both spatial and temporal integration properties with interneural delays of biological neurons. Each cell i of the network is characterized, at time t, by two components: a potential V_i^t and a binary state $X_i^t \in \{0, 1\}$. A

local parameter m_i^t, which sums up the previous spiking activities of cell i, models the membrane characteristics of cells, such as the refractory period (sodium and potassium channels), and properties of the calcium channels.

• Potential V_i^t takes into account both spatial and temporal integrations of signals, received at different sites on the membrane of cell i, over a short temporal interval Δ_{In}.

$$V_i^t = \int_{\Delta_{in}} v_i^{t-u} du \qquad with \qquad v_i^t = \sum_{j=1}^{N_i} w_{ij}^t X_j^{t-\delta_{ij}^t}$$

Signals between cells j and i are transmitted with a temporal delay $\delta_{ij}^t > 0$, function of the synaptic distance between cells j and i and are weighted by a real synaptic weight w_{ij}^t. N_i is the number of contacts between cell i and other cells. V_i^t combines the effects of signals received during a time interval $[t-\Delta_{in}, t]$.

• This model introduces for each cell i a local parameter m_i^t which sums up the spiking history of the neuron itself. m_i^t is called "spike memory term" and is a function of time. β is a constant, $0 < \beta < 1$. The evolution of m_i^t is defined by:

$$m_i^{t+1} = (1 - \beta).m_i^t + \beta.X_i^t$$

The spike memory term introduced in the model can be linked to the evolution of calcium channels. The neuron not only remembers the emission of the last spike but keep track of all the previous spikes, which is more realistic. In this model, the firing accomodation is taken into account which differs from other modelizations.

• Experiments have shown that in vitro biological neurons fire with slightly varying delays in response to repetitions of the same visual stimulus. The stochastic function π governs the probability that neuron i fires at time t, which add noise in the model. The rate of firing depends on the input currents.

The state X_i^t of a neuron is a stochastic function of potential V_i^t:

$$Proba(X_i^t = 1) = \pi_i^t(V_i^t) \qquad with \qquad \pi_i^t(u) = \frac{1}{1 + exp(-\alpha(u - m_i^{t-1}))}$$

X_i^t is equal to 1 with a probalility $\pi_i^t(V_i^t)$ and to 0 with a probability $1 - \pi_i^t(V_i^t)$. $\pi_i^t(u)$ is a sigmoïd function of slope $\alpha > 0$ with a threshold m_i^t, function of time t. Parameter α determines the amount of noise in the system.

Threshold m_i^t is also used to model the refractory period of cell i. If cell i fires at time t-1 then the firing probability of cell i at time t decreases. If cell i does not fire at time t-1 then the firing probability of cell i increases for the same value of potential u.

• The network dynamic is synchronous, and the time scale is discrete.

This neuron model can not be directly compared to the class of "integrate and fire" which models the time between two emitted spikes.

4 Modeling Visual Stimuli

The visual stimulus generated on layer 1 models light or dark moving bars of optimal direction and velocity to activate receptive fields of neurons in other layers.

The visual stimulus is periodic, corresponding to different presentations of the same signal on the retina. Activities of cells of layer 2 are high, during a temporal window D, which corresponds to the movement of the bar across their receptive fields.

$$Proba(X_i^t = 1) = \pi_i^t \simeq 1 \qquad \text{for } kT \leq t < D + kT;$$
$$Proba(X_i^t = 1) = \pi_i^t \simeq 0 \qquad \text{for } kT + D \leq t < (k+1)T$$

T is the period of the stimulus. The visual stimulus is composed of 50 presentations of the same signal ($0 \leq k < 50$).

5 Measures of synchrony

The computation of Cross Correlation Histogram (CCH) between two different spike trains help us to study the distribution and regularity of spike firing and to point out synchronization and oscillation between cells.

$$CCH_{i,j}(d) = \frac{\sum_t (X_i^t - \mu_{X_i})(X_j^{t-d} - \mu_{X_j})}{\sigma_{X_i}\sigma_{X_j}}$$

with μ_{X_i} : mean of cell X_i over time, σ_{X_i} : standard deviation of cell X_i and $0 \leq t \leq 50T$.

50 presentations of the stimulus of period T are presented on the retina. $CCH_{i,j}$ measures the correlation strength between two neurons i and j. Two cells i and j are here considered to be "strongly correlated "if $Max_d\{CCH_{i,j}(d)\} > 2/3$. The position, d_0, of the CCH peak reflects the most frequent time-difference between the coupled spikes: $d_0 = ArgMax\{CCH_{i,j}(d)\}$.

A zero-phase difference $d_0 = 0$ with a high correlation $MaxCCH_{i,j}(d_0) > 2/3$ expresses a good synchronization with no phase difference between both neurons i and j.

6 Emergence of synchronization

Emergence of synchronization occurs for some necessary parameter values of the model, with fixed and different temporal delays between vertical layers, even if left and right hemisphere areas receive visual information from the retina with different transmission delays.

One of the important questions concerning synchronization in the cortex is whether it is mediated by thalamic inputs or corticocortical connections [7]. In our model, we find that emergence of synchronization depends on the existence of connections between the two opposite layers 3L and 3R, which correspond to corticocortical connections.

Several configurations of connections (excitative, inhibitive weights) between all layers have been explored. Inhibitory connections between the two opposite layers (3L, 3R) seems to be a necessary condition for the emergence of synchronization between cells of these layers ($w_{i,j} < 0$, $w_{j,i} < 0$ for $i \in \{3L\}$, $j \in \{3R\}$). The matrix of connection signs, for all following simulations is then chosen as:

These results are consistent with other studies [6].

• In our model, the spike memory term m_i^t with $\beta \neq 0$ plays a determining role for the emergence of synchronization between neurons of the two opposite layers 3L and 3R. As β increases from 0 to an optimal value β_0, the peak position of CCH computed between two neurons of the opposite layers 3R and 3L approches

Table 1: Connectivity Matrix of the network. +/- represents excitative/inhibitive connections between two layers. Dots means that layers are not directly connected to each other.

| Layers	1	2L	2R	3L	3R
1	.	.	.	.	.
2L	+	.	.	+	.
2R	+	.	.	.	.
3L	.	+	.	.	−
3R	.	.	+	−	

zero and a reinforcement of the correlation strength is observed. The correlation strength is maximized for β_0. Neurons of opposite layers 3R and 3L also tend to be synchronous with no phase difference (figure 2). Increasing further the value of parameter $\beta > \beta_0$ leads to complex and chaotic neuronal activities.

Figure 2: CCH computed between two neurons of opposite layers 3L and 3R. As β approaches an optimal value β_0 (here 0.05), the peak of the CCH is centered at zero, neurons becomes synchronous. Parameters: $w_{3L,2L} > 0$; $w_{3R,2R} > 0$; $w_{3L,3R}, w_{3L,3R} < 0$; $\delta_{3L,2L} = 2ms$; $\delta_{3R,2L} = 5ms$; $\delta_{3L,3R} = 9ms$; $\delta_{3R,L} = 9ms$; $\Delta_{In} = 5ms$, $\alpha = 100$
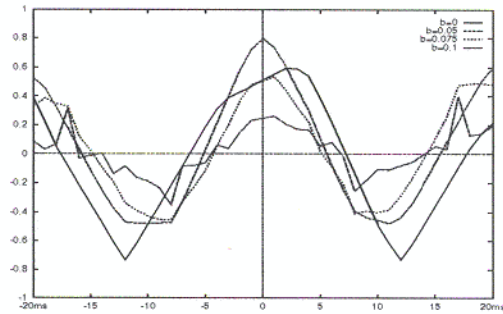
The following figure 3 presents the percentage of synchronization observed for two neurons in opposite areas 3L, 3R. Strong synchronizations with no phase-difference, up to 90 pourcent., emerge for different sets of weights or β value and are associated with high correlation strengths close to 1.

Figure 3: Percentage of synchronization for two neurons of different hemisphere for different weights and β values. High areas corrrespond to strong synchronization. Parameters: $w_{3L,2L} = 1$; $w_{3R,2R} = 1$; $w_{3L,3R} = w_{3L,3R} < 0$; $\delta_{3L,2L} = 2ms$; $\delta_{3R,2L} = 5ms$; $\delta_{3L,3R} = 9ms$; $\delta_{3R,L} = 9ms$; $\Delta_{In} = 5ms$, $\alpha = 100$
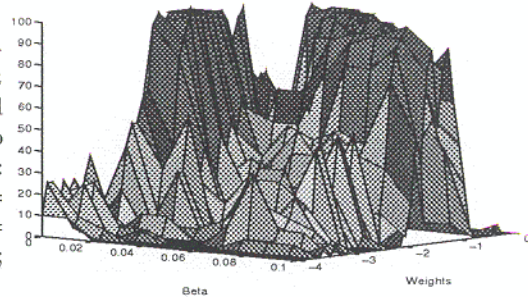
The emergence of synchronization depends on the temporal evolution of the spike memory term m_i^t for each neuron i. The optimal value β_0 which maximizes the correlation strength induces a non-linear temporal evolution.

All simulation results are independant of the initial values chosen for the spike memory term $m^{t=0}$. For $\beta = 0$, no precise synchronization is observed (left figures), and the correlation strength is low, $ArgMaxCCH_{i,j} < 2/3$. For the optimal

value, here $\beta_0 = 0.1$, the evolution of m_i^t and V_i^t induces synchronization between neurons of opposite areas 3L and 3R (right figures).

The presence of centered peaks in cross-correlograms is usually interpreted as meaning that both neurons receive directly common inputs from other sources. There is no common thalamic input to neurons located in different cortical hemispheres in our model, interhemispheric synchronization mediated here by cortico-cortical connections reproduce neurobiological observations.

7   Three types of synchronization

In the visual cortex, several synchronizations, which seem to be a universal form of correlation in the visual cortex, have been shown in the same or between different hemispheres in the work of J. Bullier's team [5]. Classification has been established using the geometrical characteristics of the central peak of the computed CCH (peak high, peak area, peak width). The more precise synchronization, "T" (for Tower), is principally characterized by a peak of great high (strong correlation strength) and a small width (good localisation in time). The less precise synchronization, called "H" (for Hill), is characterized by a large peak width (less precise synchronization). Characteristics of "C" (for castle) are intermediate between "T" and "H".

In our model, these three types of synchronization can be exhibited (figure 4) . T peaks are observed for two cells belonging to opposite areas linked by short transmission delays. H peaks are observed for two cells linked by larger transmission delays. These results can be compared to biological data which have shown that very precise temporal couplings are mediated by the direct reciprocal connections between visual cortical areas circulating through the corpus callosum (peak "T") [7]. Less precise temporal couplings are mediated by polysynaptic pathways through the corpus callosum and widely distributed over cortical regions.

Figure 4: Three types of synchronization reproduced in our model depending on various delays between cells in opposite area 3R and 3L. CCH for three couples of cells linked by cortico-cortical connections with different delays
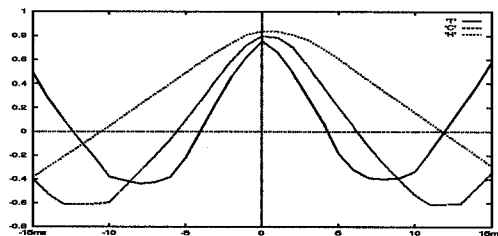
8   Statistical distribution of synchronization

● The overall network activity is then analyzed, and CCH are computed for all neuronal couples, each cell belonging to a different layer (3L or 3R). We determine how often such synchronized firing is observed by measuring the CCH peak position in the total population of neurons of the two oppostite layers 3L and 3R. Figure 5 shows the statistical distribution of peak positions which maximize the CCH function, computed for all neuronal couples belonging to distinct layers. The mathematical mode of the distributions is zero, which shows that a majority of neuronal couples tends to be synchronous.

- Simulation results were obtained here by using a 30-cells network (5 cells in layer 2L and 2R, 10 cells in layers 3L and 3R). Each cell of layer 3L (resp. 3R) receives information from one cell, randomly chosen in the precedent layer 2 and from 5 cells randomly chosen in the opposite layer 3R (resp. 3L). The statistical temporal delay distribution is gaussian. $\bar{\delta}_{A,B}$ represents here the mean of the connection delay distribution, for a cell of layer A receiving connections from a set of cells of layer B. Similar results have been obtained for larger networks. The observed frequency of synchronous cells also depends on the probabilities of connections between cells of different layers. The frequency is maximal for a high connection probability between cells of the same layer ($\simeq 0.8$) and a low, but strictly positive, connection probability between cells of opposite layers 3L and 3R. All neurons of different hemispheres 3L,3R also tend to be synchronous.

Figure 5: Histogram of position of the peak of CCH computed between all neuronal couples, each cell belonging to a distinct layer 3L or 3R. Parameters: $\beta = 0.001$ $w_{3L,2} > 0$; $w_{3R,2} > 0$; $w_{3L,3R}, w_{3L,3R} < 0$; $\bar{\delta}_{3L,2L} = 7ms$; $\bar{\delta}_{3R,2R} = 6ms$; Std of $\delta_{3L,3R}$ and $\delta_{3R,3L}$ distributions is 1ms. $\Delta_{In} = 3ms$, $\alpha = 100$
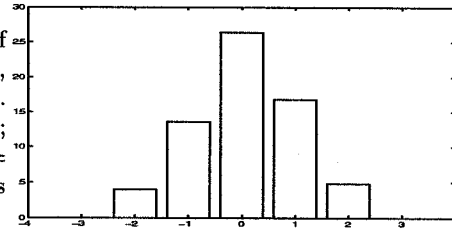
Simulation results are consistent with biological experiments which have shown that coupled spikes occuring in pairs of neurons located across different areas tend to be emitted most often at the same time [7] [3]. If the connections between layers 3L-3R are cut, no more synchronization nor oscillations are observed, as in biology.

9 Emergence of oscillations

This model gives various oscillatory correlograms (figure 6). The sharp peak and the oscillations observed are totally independent of the periodicity of the stimulus presented to the retina. The oscillation period depends on temporal delays between neurons of opposite layers, on the spike memory term m^t, and on the window of temporal integration Δ_{In}. Absence of noise in the stimulus leads to a highly regular and bursting oscillatory activity. Multiple visual stimuli (for instance bars) appear to induce synchronized oscillations in the brain. These results suggest that oscillation phase may be the "temporal code" that identifies an object as a whole. The following results reproduce these observations.

10 Modification of the visual stimuli

Generation on the retina of a sequence of images including a noise, leads to the diminution of the correlation strength, to the end of synchronization and oscillations between neurons of two opposite areas, for the same network parameters (figure 6). This shows that the observed oscillations are a response to external stimuli. This is consistent with neurobiological observations. These properties of oscillations and synchronization in the network offer possibilities for pattern recognition. Visual stimuli can also be coded by the temporal synchronization between

cells from opposite areas.

Figure 6: $CCH_{i,j}$, ($i \in 3L, j \in 3R$) is computed (p1) for a clear visual stimulus. Abolition of synchronization and oscillations with a diminution of the correlation strength is induced by various noisy stimuli (p2 with 10 pourcent of noise, p3 with 20 pourcent of noise).
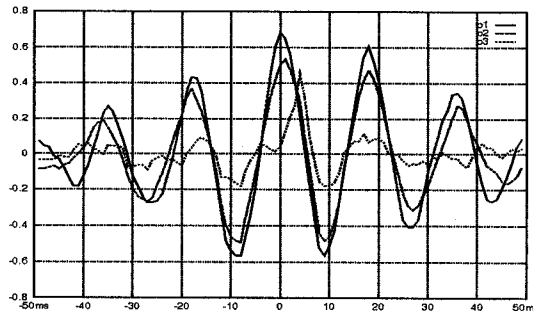
11 Conclusion

Our stochastic model with binary states simulate the behaviour of biological neurons. Its originality is to introduce a sigmoïd transition probability function, which depends not only on the potential value, but also on a local parameter which sums up the spiking history of the neuron and models the cell membrane properties (sodium, potassium, and calcium channels).

The network architecture reproduces a small part of the visual cortical areas. A chosen visual stimulus induces in the network the emergence of synchronization and oscillations between neurons, even if they receive information with different temporal delays. Our model proposes an explanation for the different types of synchronization, "T,C,H", observed in the brain, when activated by an external stimulus. Introduction of a noise in this stimulus leads to the abolition of these properties of synchronization or oscillation. These results are consistent with neurobiological observations in the visual cortex.

Acknowledgements: The author thanks R. Azencott for helpful discussions.

References

[1] B. Baird. Bifurcation and category learning in network models of oscillating cortex. *Physica*, 42:365–384, 1990.

[2] W. Gerstner and J. Leo van Hemmen. Universality in neural networks: the importance of the mean firing rate. *Biological Cybernetics*, 67:195–205, 1992.

[3] C. Gray, P. Konig, A. Engel, and W. Singer. Oscillatory responses in cat visual cortex exhibit inter-columnar synchronization which reflets global stimulus properties. *Nature*, 338(3):334–337, 1989.

[4] P. Konig, A. Engel, R. Roelfsema, and W. Singer. How precise is neuronal synchronization. *Neural Computation*, 7(3):469–485, 1995.

[5] M. Munk, L. Nowak, J. Nelson, and J. Bullier. The structural basis of cortical synchronization. 2 three types of interhemispheric coupling. *Journal of Neurophysiology*, 74(6):2401–2414, 1995.

[6] A. Nischwitz and H. Glunder. Local lateral inhibition: a key to spike synchronization? *Biological Cybernetics*, 73:389–400, 1995.

[7] L. Nowak, M. Munk, J. Nelson, A. James, and J. Bullier. The structural basis of cortical synchronization. 1. effects of cortical lesions. *Journal of Neurophysiology*, 74(6):2379–2400, 1995.

[8] J. Vibert, K. Pakdaman, and N. Azmy. Interneural delay modification synchronizes biologically plausible neural networks. *Neural Networks*, 7(4):589–607, 1994.